Review of Scientific Instruments

A new multi-channel Mach probe measuring the radial ion flow velocity profile in the boundary plasma of the W7-X stellarator

Cite as: Rev. Sci. Instrum. **90**, 033502 (2019); https://doi.org/10.1063/1.5054279
Submitted: 30 August 2018 . Accepted: 19 February 2019 . Published Online: 07 March 2019

J. Cai, Y. Liang, C. Killer, S. Liu, A. Hiller, A. Knieps, B. Schweer, D. Höschen, D. Nicolai, G. Offermanns, G. Satheeswaran, M. Henkel, K. Hollfeld, O. Grulke, P. Drews, T. Krings, and Y. Li

View Online Export Citation CrossMark

ARTICLES YOU MAY BE INTERESTED IN

Super-resolution imaging and field of view extension using a single camera with Risley prisms
Review of Scientific Instruments **90**, 033701 (2019); https://doi.org/10.1063/1.5050833

Micro-Faraday cup matrix detector for ion beam measurements in fusion plasmas
Review of Scientific Instruments **90**, 033501 (2019); https://doi.org/10.1063/1.5084219

Characteristics of the SOL turbulence structure in the first experimental campaign on W7-X with limiter configuration
Physics of Plasmas **25**, 072502 (2018); https://doi.org/10.1063/1.5033353

Challenge us.
What are your needs for periodic signal detection?
Watch

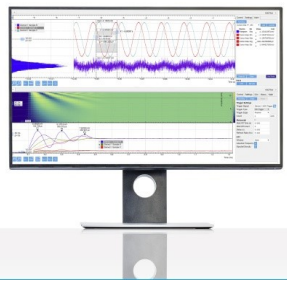

Zurich Instruments

© 2019 Author(s).

Review of Scientific Instruments ARTICLE scitation.org/journal/rsi

A new multi-channel Mach probe measuring the radial ion flow velocity profile in the boundary plasma of the W7-X stellarator

Cite as: Rev. Sci. Instrum. 90, 033502 (2019); doi: 10.1063/1.5054279
Submitted: 30 August 2018 • Accepted: 19 February 2019 •
Published Online: 7 March 2019

View Online Export Citation CrossMark

J. Cai,[1,2,3,a] Y. Liang,[3] C. Killer,[4] S. Liu,[1,3] A. Hiller,[3] A. Knieps,[3] B. Schweer,[3] D. Höschen,[3] D. Nicolai,[3] G. Offermanns,[3] G. Satheeswaran,[3] M. Henkel,[3] K. Hollfeld,[3] O. Grulke,[4] P. Drews,[3] T. Krings,[3] and Y. Li[1,3]

AFFILIATIONS

[1]Institute of Plasma Physics, Chinese Academy of Sciences, P.O. Box 1126, Hefei 230031, People's Republic of China
[2]University of Science and Technology of China, Hefei 230026, People's Republic of China
[3]Forschungszentrum Jülich GmbH, Institut für Energie-und Klimaforschung–Plasmaphysik, Partner of the Trilateral Cluster (TEC), 52425 Jülich, Germany
[4]Max-Planck-Institut für Plasmaphysik Teilinstitut Greifswald, Wendelsteinstr. 1, 17491 Greifswald, Germany

[a]E-mail: jqcai@ipp.ac.cn

ABSTRACT

Ion flow velocity measurement in the edge and scraper-off layer region is beneficial to understand the confinement related phenomenon in fusion devices such as impurity transport and plays an important role in impurity control. During the Wendelstein 7-X (W7-X) operation phase 1.2a, a multi-channel (MC) Mach probe mounted on the multi-purpose manipulator has been used to measure radial profiles of edge ion flow velocity. This MC-Mach probe consists of two polar and two radial arrays of directional Langmuir pins (28 pins in total) serving for different aims, of which the polar arrays could obtain a polar distribution of ion saturation current, while the radial arrays can be used to study the dynamic process of a radially propagated event. In this paper, we report the observation of the radially outward propagation of a low frequency mode with a speed of around 200 m/s. The first measurement of the radial ion flow velocity profile using the MC-Mach probe in the boundary plasma of the W7-X with an island divertor will also be presented.

Published under license by AIP Publishing. https://doi.org/10.1063/1.5054279

I. INTRODUCTION

Ion flow velocity measurement in the edge and scraper-off layer (SOL) region is of benefit to understand the confinement related phenomenon in fusion devices such as impurity transport[1] and plays a crucial role in impurity control.[2] A lot of attempts have been made to measure the ion flow velocity, including Doppler shift measurement of impurity lines[3,4] and probe measurement,[5] in which the Mach probe[6] is the cheapest and simplest one. In general, the most common Mach probe is a parallel Mach probe aligned to magnetic field lines, consisting of two directional pins mounted on the opposite side of an insulator. The parallel Mach number (the ratio of parallel ion flow velocity to ion sound speed) can be deduced from the ratio of the upstream to the downstream ion saturation current collected by probe pins.[5] A more complex Mach probe is a Gundestrup Mach probe consisting of several directional pins mounted around an insulator at the different angle.[7] In addition to the parallel flow, the perpendicular (poloidal) flow caused by $\vec{E} \times \vec{B}$ drift will exist as well in the case of a strong radial electric field in the edge and SOL region. This setup allows to measure the perpendicular Mach number since the ion saturation current collected by inclined pins is sensitive to the perpendicular flow.

Wendelstein 7-X (W7-X), one of the world's largest and most advanced stellarators, has an intrinsic magnetic island chain at the boundary and aims for the demonstration of high performance steady-state plasma operation. The effect of magnetic islands on plasma flow has been demonstrated, and the phenomenon that the perpendicular flow reverses at the center of the magnetic island has

Published under license by AIP Publishing

been observed on LHD[8] and TJ-II.[9] To study the effect of magnetic islands of W7-X on plasma flow, a multi-array Mach probe, which includes 8 rows in the radial direction and 28 pins in total, has been successfully commissioned and put into use on W7-X.

The rest of this paper is organized as follows: the related diagnostic setup will be presented in Sec. II, followed by the presentation of the preliminary measurement of the radial ion flow velocity profile in Sec. III. The discussion and conclusion will be given in Sec. IV.

II. DIAGNOSTIC SETUP

W7-X is equipped with a multi-purpose manipulator (MPM) system,[10] which acts as a carrier system for various probe heads. It is located near the outer midplane of module four at flange AEK40 (toroidal angle 200.7°), as Fig. 1 shows. A new probe interface with a base adapter has been used to exchange various probe heads easily, and the probe head can be mounted on the base adapter, which can be fixed by a knurled on the manipulator system.[10] The MPM system is able to insert the probe head into the plasma edge with a maximum stroke depth of 350 mm and a maximum acceleration of 30 m/s^2, both of which could be controlled and adjusted by a Programmable Logic Controller (PLC) system,[11] making it possible to measure the radial profile within the SOL region as well as crossing the last closed flux surface (LCFS). For this campaign, the stroke position in terms of major radius is 6.06-6.08 m, which is limited by the hazard of arc striking. When the probe head is plunged too deep in a high performance discharge, the ion saturation current collected by the front pins will increase rapidly to more than 10 A, which can be harmful to electronic elements. Laser sensors have been used to monitor the position of the probe head during plunging with an uncertainty of 0.2 mm.

As Fig. 2(a) shows, the probe head is constructed in the shape of a cylinder whose diameter of cross section is 42 mm and total length is 79 mm. There are 28 pins made of tungsten located around the cylindrical rod because of its high resistance to heat loads. As seen in Fig. 2(b), these pins are flush mounted to the surface of the probe head cover instead of standing proud in the plasma, which enables the pins to collect the ion saturation current directionally. Each pin is isolated from its radially adjacent pins by an isolator between them, and the radial distance between adjacent pins is 6 mm. The area of each pin is approximately 11 mm^2, and the effective collecting areas of two pins in the opposite side are supposed to be identical. Thus, in the later calculation, the ratio of saturation current density could be replaced by the ratio of saturation current.

For a simple parallel Mach probe, there are only two directional pins located in the opposite side. In this Mach probe head, 8 pins are evenly located around the cylindrical rod in the first two rows, respectively, working as a Gundestrup Mach probe. This setup is able to obtain the polar distribution of ion saturation current, and consequently the perpendicular and parallel ion flow velocity can be deduced.[7] Another 12 pins are radially mounted in 6 rows back to back, measuring a radial profile of ion flow velocity simultaneously. The radial array, as one of the characteristics of this Mach probe head, could also be used to study the dynamic process of radially propagated events, such as bursts, modes caused by MHD instabilities, and the perturbation of density and temperature caused by modulations.

A probe head cover made of graphite has been used to protect the interior part from the unwanted direct contact with plasma, as shown in Fig. 2(b). Graphite has been chosen because of its high heat resistance, by which it could protect the interior part against the high heat loads from the hot plasma, especially those caused by electron cyclotron resonance heating (ECRH) stray radiation, and of its good mechanical stability under a high acceleration. However, in this campaign, the graphite cover has been observed to be more likely to give rise to arc striking, which has limited the plunge depth of the probe head. For this reason, boron nitride has been chosen as the material of the Mach probe head instead of graphite for the next campaign operation phase 1.2b (OP1.2b).

To perform ion saturation current measurements, a biasing voltage of −160 V with respect to the W7-X plasma vessel is applied to these pins, provided by integrated capacitor arrays in which one

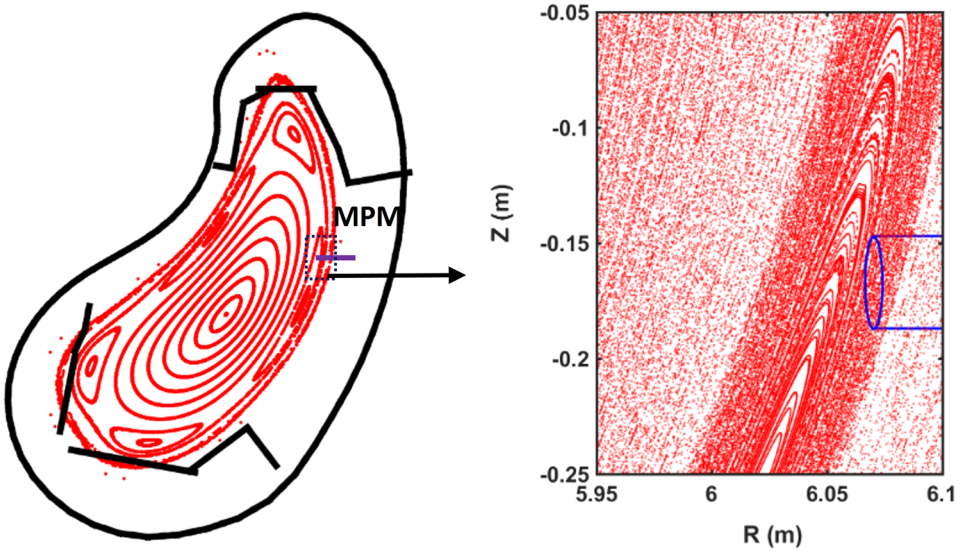

FIG. 1. The Poincare diagram at toroidal angle 200.7° in the standard configuration EJM on W7-X. The position of the multi-purpose manipulator in the discharge #171206025 is labeled by the blue line, and the black lines represent divertor targets and the outer vacuum vessel. The size of probe head relative to the size of the magnetic island could be seen from the enlarged drawing of the island region.

Published under license by AIP Publishing

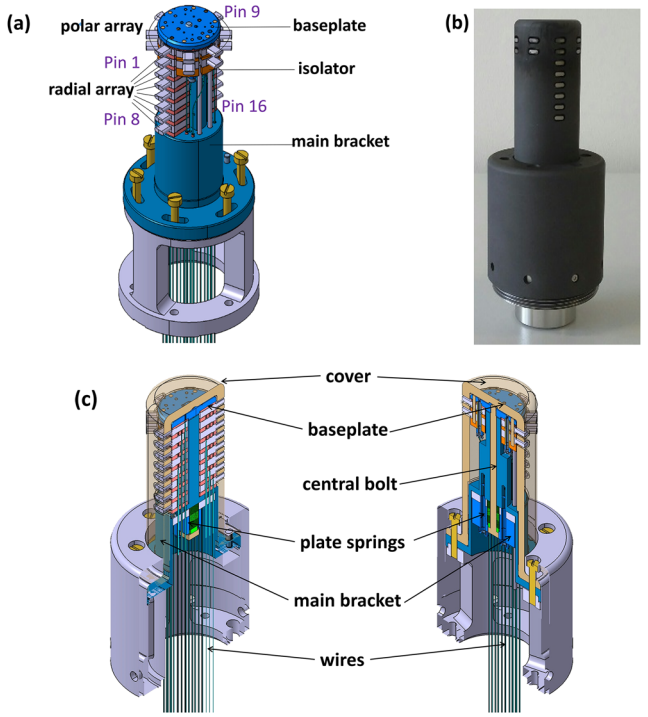

FIG. 2. Design of the Mach probe head without cover (a), the picture of the Mach probe head (b), and the cutaway views of the Mach probe head (c). The orange parts are isolators, and the silver parts are pins. Some pins have been labeled in the diagram by blue text. The pins of radial array seen in the diagram are labeled 1-8 from top to bottom, and the pins on the opposite are labeled 9-16. The pins in the first polar array are labeled 1, 18, 20, 22, 9, 23, 26, and 27 counterclockwise, while the pins in the second array are labeled 2, 17, 19, 21, 10, 24, 25, and 28.

unit is used to bias four Mach pins, as shown in Fig. 3. The ion saturation current signal is converted into the voltage signal by using a pre-amplifier with a gain factor from 0.1 V/A up to 1000 V/A, which could be adjusted depending on the magnitude of the saturation current. A 32-channel data acquisition system with 2 MHz sampling rate and 14 bit effective resolution has been used to convert the voltage signal to digital numeric values. An isolation amplifier has been used to isolate each channel of the probe system from the data acquisition system for the aim of avoiding grounding problems and to allow shunt measuring at high potential.

III. THE MODEL FOR MACH PROBE INTERPRETATION

The Mach number can be expressed as an exponential form of the ratio of the upstream ion saturation current density to the downstream ion saturation current density,

$$J_{up}/J_{down} = \exp(KM_{//}), \quad (1)$$

which has been demonstrated theoretically and experimentally.[5,12–14] In these fluid models of the Mach probe, the formula has the same exponential form, while the calibration factor K is varied depending on the various plasma parameters, such as ion temperature,[5] viscosity,[13,14] and collisionality.

The magnetic field in the edge region on W7-X is 2.2–2.3 T, and the ion Larmor radius is around 0.19 mm,[15] much smaller than the size of Mach probe pins 2 mm. As a consequence, the theory of magnetized plasma is suitable to interpret the experiment data on W7-X. Moreover, in the experiment on W7-X, not only the parallel Mach number but also the perpendicular one is of interests to us. Therefore, a fluid model in magnetized plasma which takes account of the perpendicular drift has been used to deduce the parallel and also perpendicular Mach numbers.[16] The formula is given as

$$J_{up}/J_{down} = \exp[K(M_{//} - M_{\perp}\cot\theta)], \quad (2)$$

where θ is the angle between the magnetic field line and the collecting surface of pins, and the calibration factor K lies between 2.3 and 2.5. Similar formula has also been given by another 2D fluid model using a self-similar method,[17,18] which indicates the same exponential form and the difference between the two formulas is the calibration factor K = 2 in the latter 2D fluid model. In this paper, K is always taken as K = 2.5 when deducing the Mach number.

Equation (2) shows that the parallel Mach number could be deduced directly from the ratio of currents measured by the pins whose collecting surface is perpendicular to the field lines (θ = 90°), while another ratio of currents measured by pins with a different orientation angle is required for the deduction of the perpendicular Mach number. In the previous experiments on the CASTOR (Cezch Academy of Sciences TORus) tokamak,[19] it has been demonstrated that this model fits well with the measurements, while θ lies between 30° and 150°, so the pins 19, 25, 20, and 26 (θ = 0°) have been excluded for the data interpretation. In addition, the pins 18, 22, and 24 in the polar arrays have been open circuited during the assembling. As a consequence, the perpendicular Mach number cannot be deduced by the pins in the first row because of the defective relevant pins used for deducing, while the perpendicular Mach number can be deduced from the difference between the ratio of currents

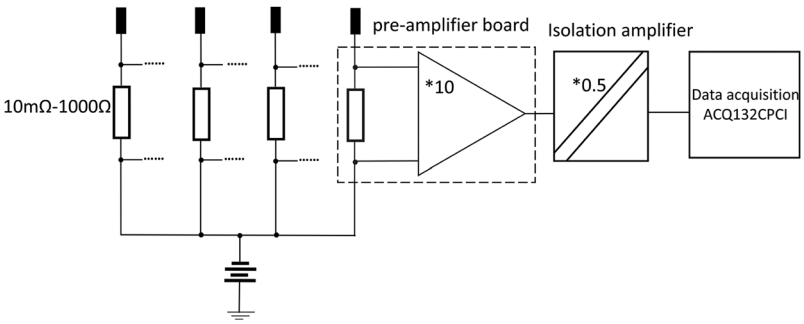

FIG. 3. The simplified circuit diagram of Mach probe. In this circuit diagram, the amplifiers and the data acquisition system of the first three pins are omitted.

Published under license by AIP Publishing

measured by pin 2–pin 10 and that measured by pin 21–pin 28 in the second row,

$$M_{//} = \frac{\ln R_1}{K}, R_1 = J_2/J_{10}, \quad (3)$$

$$M_{\perp} = \frac{\ln R_1}{K} - \frac{\ln R_2}{K}, R_2 = J_{21}/J_{28}. \quad (4)$$

Since the field line is not strictly perpendicular to the collecting surface of the radial array on this experiment, the effect of misalignment on parallel and perpendicular flow should be taken into consideration. The effect of misalignment on flow velocity has been given analytically,[19]

$$M_{\perp}^{*} \approx M_{\perp},$$
$$M_{//}^{*} \approx M_{//} - M_{\perp}\Delta\theta, \quad (5)$$

where the Mach number with a star superscript is the actual value of the Mach number and $\Delta\theta$ is the angle misalignment. The misalignment has a little effect on the perpendicular flow velocity, while it could affect the parallel flow speed only if the product of perpendicular flow and the misalignment angle is big enough. In the standard configuration, the incident field line angle at the stroke position is around 5° (0.09 rad); consequently, the effect of the misalignment on the flow speed is negligible.

IV. PRELIMINARY EXPERIMENT RESULTS

The Mach probe head has been successfully commissioned and used at the recent experiment of operation phase 1.2a (OP1.2a) campaign on W7-X. Figure 4 shows the basic parameters of discharge #171206025 at this campaign, whose magnetic configuration is EJM (standard configuration with five independent magnetic islands in the edge) with the magnetic field direction being reversed compared to the default setup, indicating that the direction of toroidal magnetic field is clockwise when viewing from the top.

Pellet injection has been used at the end of the discharge; consequently, there is a remarkable increase in the electron density and a decrease in the electron temperature. The probe head has been plunged into the plasma edge twice, and the analysis of the data during the first plunge could be seen in Fig. 6. During the first plunge, the Electron Cyclotron Resonance Heating (ECRH)[20] heating power is 1 MW, line-integrated density measured by interferometry[21] is 2.15×10^{19} m^{-3}, and the core electron temperature measured by Electron Cyclotron Emission (ECE)[22] diagnostic is 1.8 keV.

Figure 5 shows the raw and filtered data of ion saturation current from pin 1 to pin 4 during the first plunge in discharge #171206025, of which a low pass filter with a cut-off frequency of 300 Hz has been used to smooth the raw saturation current signal. The ion saturation current of pin 4 is much lower than that of pin 1, indicating a quick decay of ion saturation current along the radial direction, which could be seen in Fig. 6(a) as well.

Figure 6 shows the measurement of radial profiles of the ion saturation current and Mach number during the first plunge in discharge #171206025. As seen from Fig. 6(a), the profiles of ion saturation current from pin 1 to pin 4 show a good repeatability. When the distance is greater than 6.09 m, the value of ion saturation current becomes insignificant because of the low ion density and temperature there. Since the parallel Mach number is determined by the ratio of current density, the precision of the Mach number would be strongly affected by deviations of measurement when the current signal is low, which could be seen in Fig. 6(b). The radial profiles of

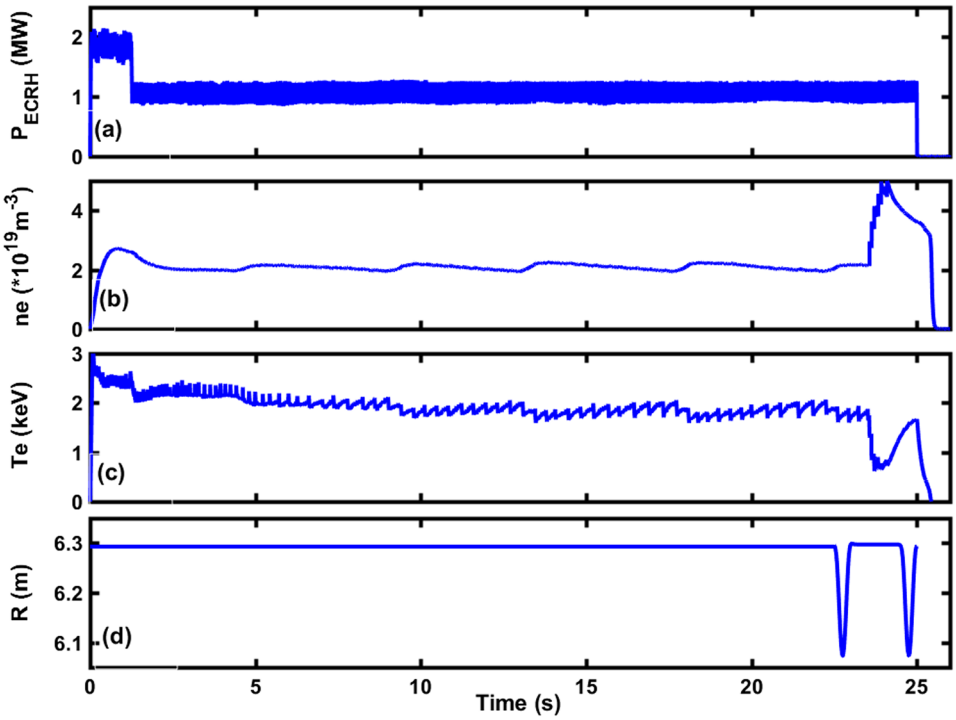

FIG. 4. Main parameters of shot #171206025. The diagram from the top to bottom is ECRH heating power (a), the core line-integrated density measured by interferometry (b), the core electron temperature measured by ECE (c), and the position of the Mach probe head (d).

Published under license by AIP Publishing

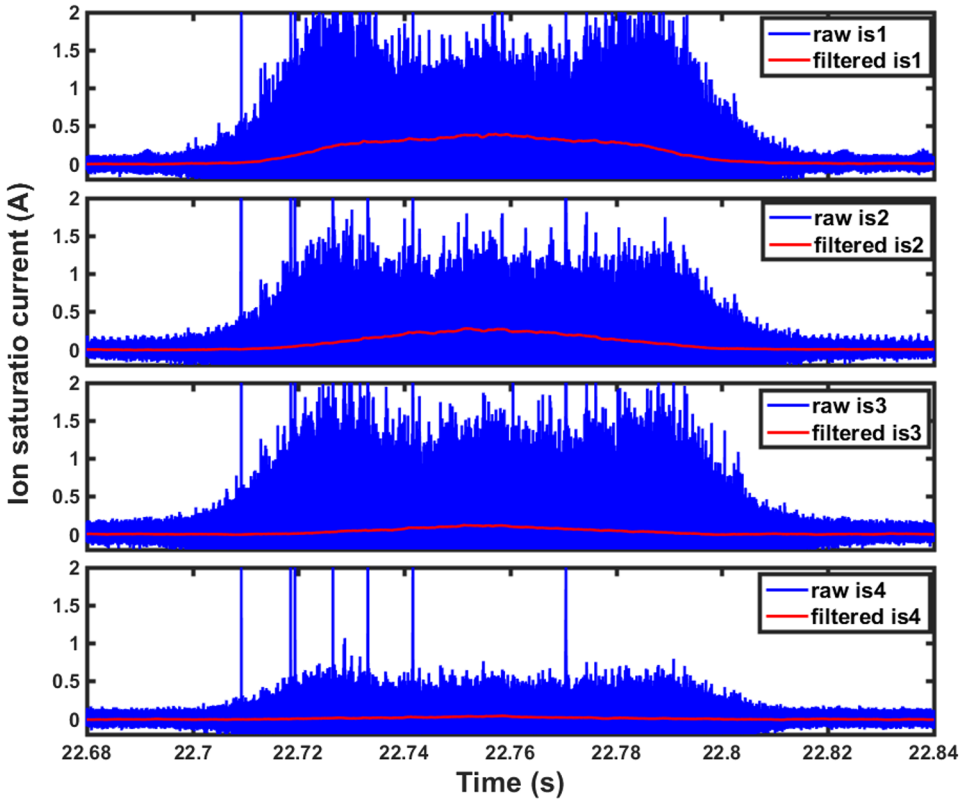

FIG. 5. The raw and filtered data of ion saturation current from pin 1 to pin 4 during first discharge in discharge #171206025.

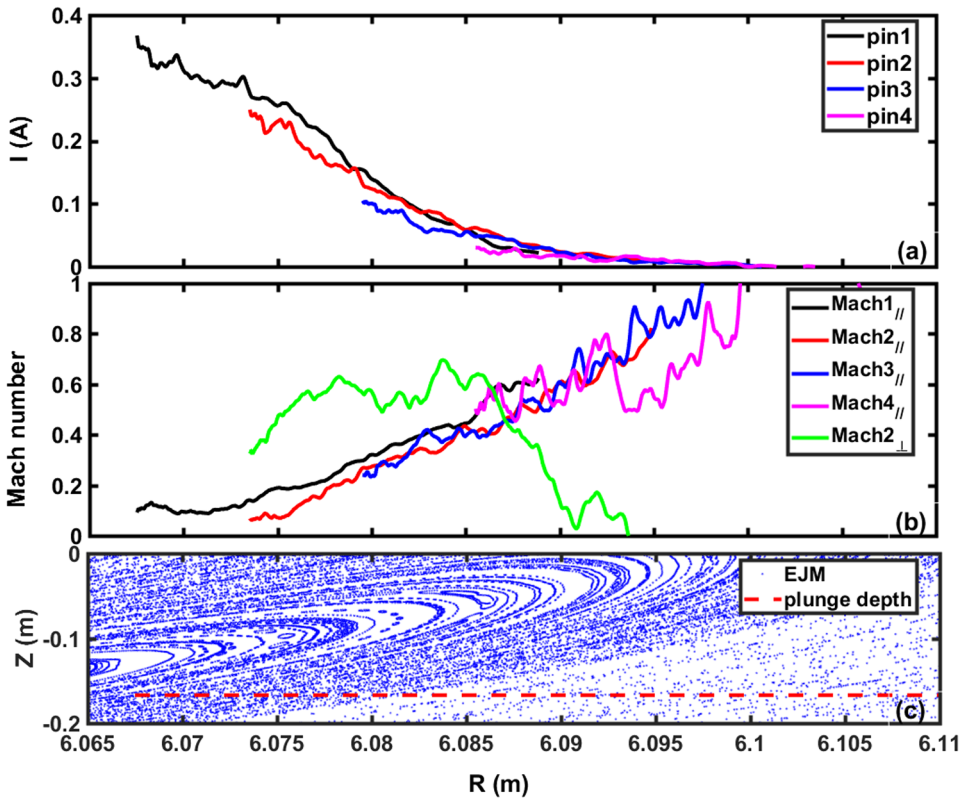

FIG. 6. The result of shot #171206025. The diagrams from the top to bottom are the radial profiles of ion saturation current from pin 1 to pin 4 (a), the radial profiles of perpendicular and parallel Mach numbers (b), and the Poincare picture of the island regime in the EJM configuration (c).

Published under license by AIP Publishing

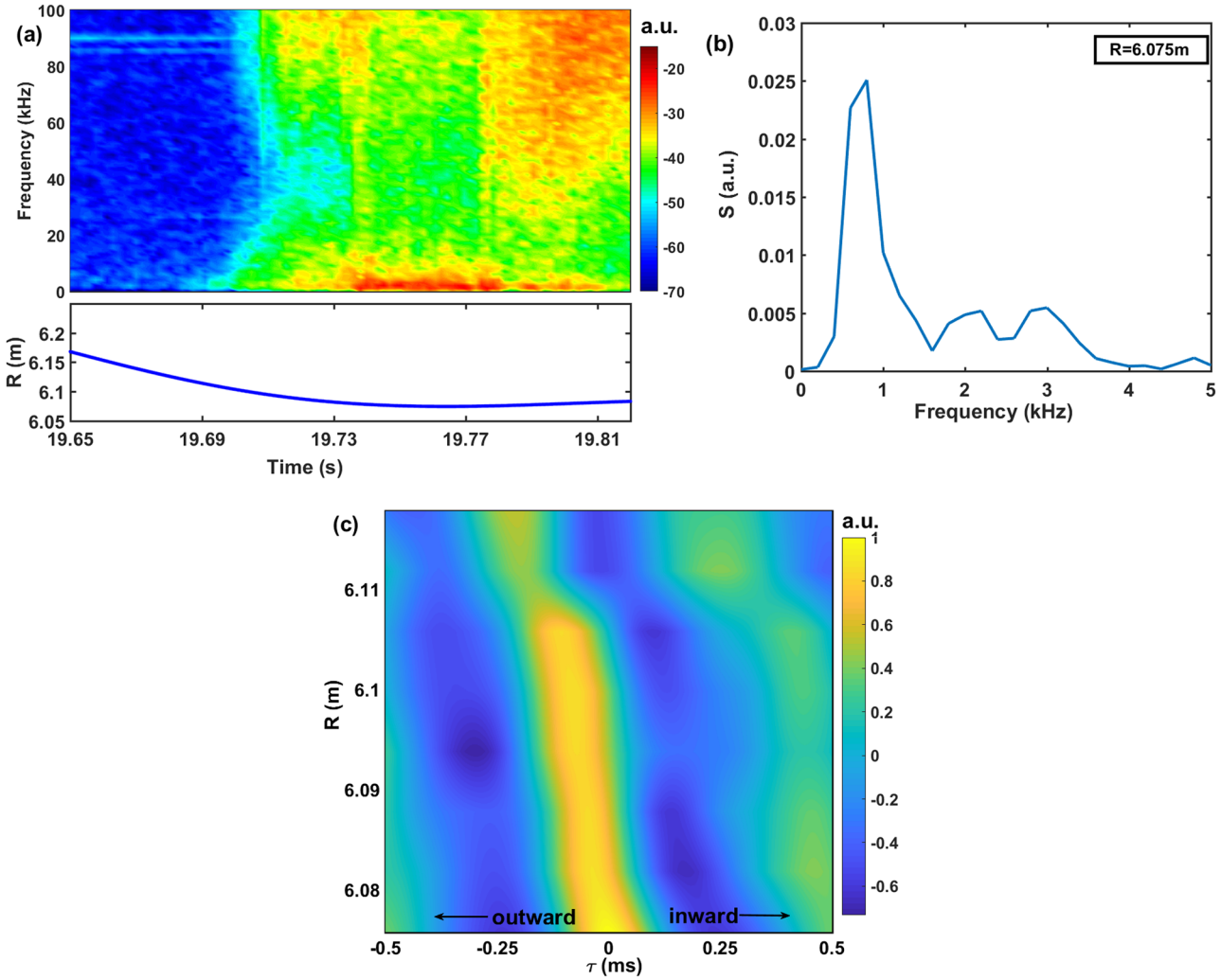

FIG. 7. (a) The autopower spectrum of pin 9 in discharge #171205027, (b) the frequency spectrum of pin 9 at R = 6.075 m, and (c) the cross correlation between the 0.5-5 kHz band-pass filtered signal measured by pin 9 with those measured by other radial pins 9-16, which indicates that the low frequency mode propagates outwardly with a speed of around 200 m/s.

the parallel Mach number deduced from the pins of first four rows show the same monotonically increasing trend and a good repeatability as the profiles of ion saturation current do, whereas when the distance is greater than 6.09 m, the profiles do not overlap very well. The perpendicular Mach number in the first row is missing because of the defective relevant pins used for deducing. The parallel flow direction is clockwise when viewing from the top, and the perpendicular flow direction is downward.

Figure 7(a) is the autopower spectrum of pin 9 in the discharge #171205027, and a low frequency mode can be observed when the probe is inserted into the plasma deep enough (R < 6.10 m). A similar low frequency mode has been observed during the first operational phase (OP1.1) on W7-X.[23] Figure 7(b) is the frequency spectrum of pin 9 at R = 6.075 m, which shows that the peak frequency of this low frequency mode is around 1 kHz. To study the radial propagation of this low frequency mode, the relevant component of this signal has been extracted using a 0.5-5 kHz band-pass filter. Figure 7(c) shows the cross correlation of the 0.5-5 kHz band-pass filtered signal of pin 9 with those measured by the entire radial array (pin 9–pin 16), and a clear radially outward propagation with a velocity of around 200 m/s can be seen.

V. DISCUSSION AND CONCLUSION

In addition to the radial propagation of the modes with different frequencies, the dynamic process of the density perturbation caused by modulations is also one of the major research objects of the Mach probe head. Future experiments in the second divertor campaign on W7-X (OP1.2b) will include the analysis of the radial propagation of the density perturbation induced by gas puffs,

Published under license by AIP Publishing

which can be well studied using the radial array of the Mach probe.

During the assembling, the pins with a quasi-rectangular cross section do not fit well with the slots, which makes the loosened pins and wires squeeze each other. Although several pins of polar arrays are open circuited because of the fragile wires being broken, the results of the perpendicular and parallel Mach numbers are less affected. For future experiments in the second divertor campaign on W7-X (OP1.2b), a new inner-side design will be used to make the assembly process more robust. Moreover, a new Mach probe head whose cover is made of insulated boron nitride instead of graphite has been designed to reach deeper plunges which will then allow us to assess plasma flow in the entire island. In addition, a gas feeding pipe has also been applied to the new Mach probe head to allow for gas puffing.

In conclusion, the multi-channel Mach probe head has been successfully commissioned and put into use on W7-X OP1.2a campaign, and the radial profile of parallel and perpendicular flow velocity has been obtained by the Mach probe head. The dynamic process of radially propagated mode has also been studied by the radial array of the Mach probe head, and a low frequency mode propagating outward with a speed of around 200 m/s has been observed.

ACKNOWLEDGMENTS

This work has been carried out within the framework of the EUROfusion Consortium and has received funding from the EURATOM research and training programme 2014–2018 under Grant Agreement No. 633053. The views and opinions expressed herein do not necessarily reflect those of the European Commission. The support provided by the China Scholarship Council (CSC), the National Natural Science Foundation of China (Grant No. 51828101), and the K. C. Wong Education Foundation is acknowledged. Finally, the support by W7-X Team is acknowledged as well.

REFERENCES

[1] R. C. Isler, Nucl. Fusion **23**, 1017 (1983).
[2] J. Neuhauser, W. Schneider, and R. Wunderlich, Nucl. Fusion **24**, 39 (1984).
[3] M. G. Bell, Nucl. Fusion **19**, 33 (1979).
[4] S. Suckewer, H. P. Eubank, R. J. Goldston, E. Hinnov, and N. R. Sauthoff, Phys. Rev. Lett. **43**, 207 (1979).
[5] M. Hudis and L. M. Lidsky, J. Appl. Phys. **41**, 5011 (1970).
[6] K.-S. Chung, Plasma Sources Sci. Technol. **21**, 063001 (2012).
[7] C. S. MacLatchy, C. Boucher, D. A. Poirier, and J. Gunn, Rev. Sci. Instrum. **63**, 3923 (1992).
[8] K. Ida, N. Ohyabu, T. Morisaki, Y. Nagayama, S. Inagaki, K. Itoh, Y. Liang, K. Narihara, A. Y. Kostrioukov, B. J. Peterson, K. Tanaka, T. Tokuzawa, K. Kawahata, H. Suzuki, and A. Komori, Phys. Rev. Lett. **88**, 015002 (2002).
[9] T. Estrada, E. Ascasíbar, E. Blanco, A. Cappa, C. Hidalgo, K. Ida, A. López-Fraguas, and B. P. van Milligen, Nucl. Fusion **56**, 026011 (2016).
[10] D. Nicolai, V. Borsuk, P. Drews, O. Grulke, K. P. Hollfeld, T. Krings, Y. Liang, C. Linsmeier, O. Neubauer, G. Satheeswaran, B. Schweer, and G. Offermanns, Fusion Eng. Des. **123**, 960 (2017).
[11] G. Satheeswaran, K. P. Hollfeld, P. Drews, D. Nicolai, O. Neubauer, B. Schweer, and O. Grulke, Fusion Eng. Des. **123**, 699 (2017).
[12] P. C. Stangeby, Phys. Fluids **27**, 2699 (1984).
[13] K. S. Chung, Phys. Plasmas **1**, 2864 (1994).
[14] I. H. Hutchinson, Phys. Rev. A **37**, 4358 (1988).
[15] P. Drews, Y. Liang, S. Liu, A. Krämer-Flecken, O. Neubauer, J. Geiger, M. Rack, D. Nicolai, O. Grulke, C. Killer, N. Wang, A. Charl, B. Schweer, P. Denner, M. Henkel, Y. Gao, K. Hollfeld, G. Satheeswaran, N. Sandri, and D. Höschen, Nucl. Fusion **57**, 126020 (2017).
[16] H. Van Goubergen, R. R. Weynants, S. Jachmich, M. Van Schoor, G. Van Oost, and E. Desoppere, Plasma Phys. Controlled Fusion **41**, L17 (1999).
[17] I. H. Hutchinson, Phys. Rev. Lett. **101**, 035004 (2008).
[18] I. H. Hutchinson, Phys. Plasmas **15**, 123503 (2008).
[19] J. P. Gunn, C. Boucher, P. Devynck, I. Ďuran, K. Dyabilin, J. Horaček, M. Hron, J. Stöckel, G. Van Oost, H. Van Goubergen, and F. Žáček, Phys. Plasmas **8**, 1995 (2001).
[20] V. Erckmann, P. Brand, H. Braune, G. Dammertz, G. Gantenbein, W. Kasparek, H. P. Laqua, H. Maassberg, N. B. Marushchenko, G. Michel, M. Thumm, Y. Turkin, M. Weissgerber, and A. Weller, Fusion Sci. Technol. **52**, 291 (2017).
[21] K. J. Brunner, T. Akiyama, M. Hirsch, J. Knauer, P. Kornejew, B. Kursinski, H. Laqua, J. Meineke, H. Trimiño Mora, and R. C. Wolf, J. Instrum. **13**, P09002 (2018).
[22] S. Schmuck, H. J. Hartfuss, M. Hirsch, and T. Stange, Fusion Eng. Des. **84**, 1739 (2009).
[23] S. C. Liu, Y. Liang, P. Drews, A. Krämer-Flecken, X. Han, D. Nicolai, G. Satheeswaran, N. C. Wang, J. Q. Cai, A. Charl, J. Cosfeld, G. Fuchert, Y. Gao, J. Geiger, O. Grulke, M. Henkel, M. Hirsch, U. Hoefel, K. P. Hollfeld, D. Höschen, C. Killer, A. Knieps, R. König, O. Neubauer, E. Pasch, K. Rahbarnia, M. Rack, N. Sandri, S. Sereda, B. Schweer, E. H. Wang, Y. L. Wei, G. Weir, and T. Windisch, Nucl. Fusion **58**, 046002 (2018).

Published under license by AIP Publishing